TAM 554- Lecture #3 Elastic and Plastic Deformation of Materials: Stress and Strain Tensors

Plasticity deals with calculation of stresses in a body, (ductile material) permanently de by a set of applied forces. Unlike elastic solids in which the state of strain depends only final state of stress, the deformation that occurs in a plastic solid in determined by the cc history of loading. The plasticity is therefore incremental (the final distortion is the incremental distortion following the loading path).

An annealed metal may be regarded homogenous (no holes etc.) and isotropic (same pr in different directions) if the crystal grains are distributed with random orientations. Upon deformation crystallographic directions rotate to a common axis, producing preferred orie

In many cases, it is customary to assume that material remains isotropic. In ductile metals deformation can continue to large strains without failure. Large strains occur in metal v processes, in the vicinity of cracks and voids during ductile fracture. Very little conside has been given to elasto-plastic problems in which plastic strains are of the same o magnitude as elastic strains. Furthermore, in many problems perfect plasticity is assumed materials strain hardening occurs and needs to be accounted for.

True Stress-Strain Curve

Stress - Strain curve in tension and compression coincide if true stress σ is plotted against (or natural) strain ε.

$$\sigma = \frac{P}{A} = \text{current load / current crossectional area}$$

$$d\varepsilon = \frac{d\ell}{\ell} = \text{change in length / current length.}$$

$$\varepsilon = \ell n\left(\frac{\ell}{\ell_o}\right);\ \ell_o = \text{original length},\ \ell = \text{current length}.$$

$$= \text{logarithmic strain}$$

$$e = \text{engineering strain} = \frac{\Delta\ell}{\ell_o}$$

$$\varepsilon = \ell n(l + e)$$

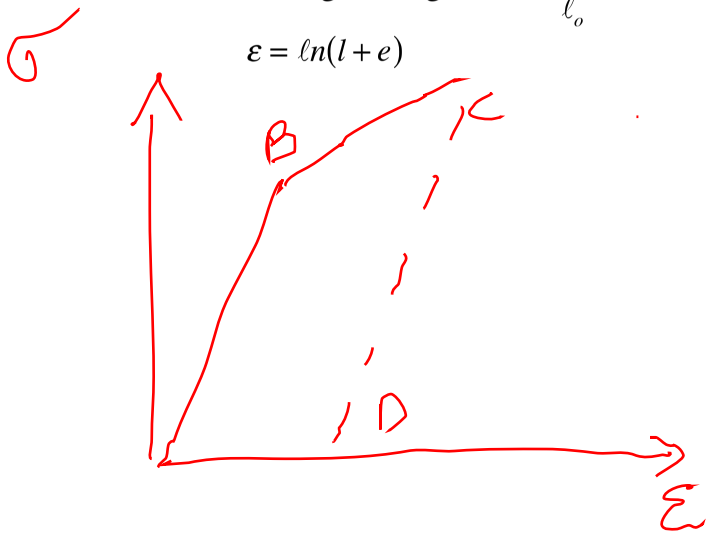

$B =$ location yield (an arbitrary definition needed) generally defined as a small plastic strain offset

σ_y = yield stress

For theoretical considerations, it is generally assumed that a sharp yield point exists, ie. ela strain = total strain up to B.

If the specimen is stressed to some point C in the plastic range and unloaded elastic recover occurs along path CD.

Stress-Strain Curve Representations

$$\left.\begin{array}{l} \varepsilon^P = \varepsilon - \dfrac{\sigma}{E} \quad \varepsilon = Total \\ \dfrac{\sigma}{E} = elastic \\ \varepsilon^P = plastic \end{array}\right\} strains$$

H = slope of stress-strain curve excluding the elastic strain.

T = slope of the curve including the elastic strain for a given value of stress σ.

H = Plastic Modulus.

T = Tangent Modulus.

E = Elastic Modulus.

Increment of stress $d\sigma$ produces an elastic strain increment $d\sigma/E$ and a plastic strain incre
$d\sigma/H$. The total strain increment is $d\sigma/T$.

$$\frac{1}{T} = \frac{1}{E} + \frac{1}{H}$$

T = Tangent Modulus

H = Plastic Modulus

E = Elastic Modulus

$H >> T$ $\qquad \varepsilon \approx \varepsilon_y \qquad \dfrac{1}{T} \approx \dfrac{1}{E}$

$H \approx T$ $\qquad \varepsilon >> \varepsilon_y \Leftrightarrow$ elastic strain increment is negligible compared to plastic strain increment.

Material with $E \Rightarrow \infty$ is called rigid plastic. It remains undeformed as long as the stress is b
the yield point.

Lateral contraction occurs in a tensile test.

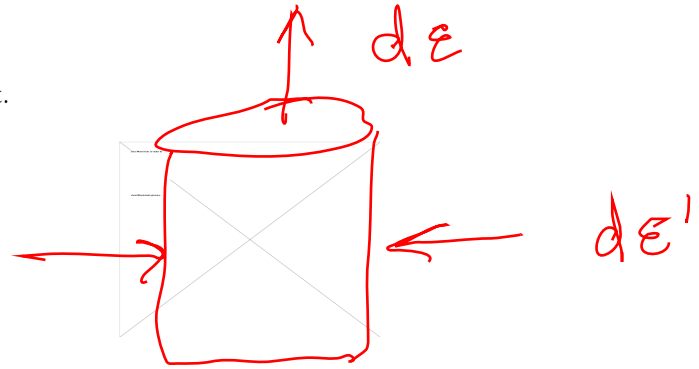

$$\eta = \text{Contraction ratio} = \frac{\text{lateral strain increment}}{\text{longitudinal strain increment}} = -\frac{d\varepsilon'}{d\varepsilon}$$

In the elastic region, contraction ratio = ν= Poisson's ratio. In the plastic region the plasti
of the lateral strain increment is equal to half the longitudinal plastic strain increment.

$$d\varepsilon' = d\varepsilon^{e'} + d\varepsilon^{p'}$$

$$= -\nu d\varepsilon^{e} - \frac{1}{2} d\varepsilon^{p} = -\nu d\varepsilon^{e} - \frac{1}{2}\left(d\varepsilon - d\varepsilon^{p}\right)$$

$$d\varepsilon' = -\frac{1}{2} d\varepsilon + \left(\frac{1}{2} - \nu\right) d\varepsilon^{e}$$

Note: $d\varepsilon = d\sigma/T$

$$d\varepsilon^{e} = \frac{d\sigma}{E} = \left(\frac{T}{E}\right) d\varepsilon$$

Contraction ratio

$$\eta = -\frac{d\varepsilon'}{d\varepsilon} = \frac{1}{2} - \left(\frac{1}{2} - \nu\right)\frac{T}{E}$$

As deformation proceeds $T \to 0$ $\eta \to 1/2$.

$$T = \frac{d\sigma}{d\varepsilon} \qquad \frac{d\sigma}{d\varepsilon} \to 0 \Rightarrow T = 0$$

Empirical stress-strain equations.

Ludwik power law: $\sigma = C\,\varepsilon^{n}$ (rigid plastic material) $\varepsilon \approx \varepsilon^{p}$ no elastic region.

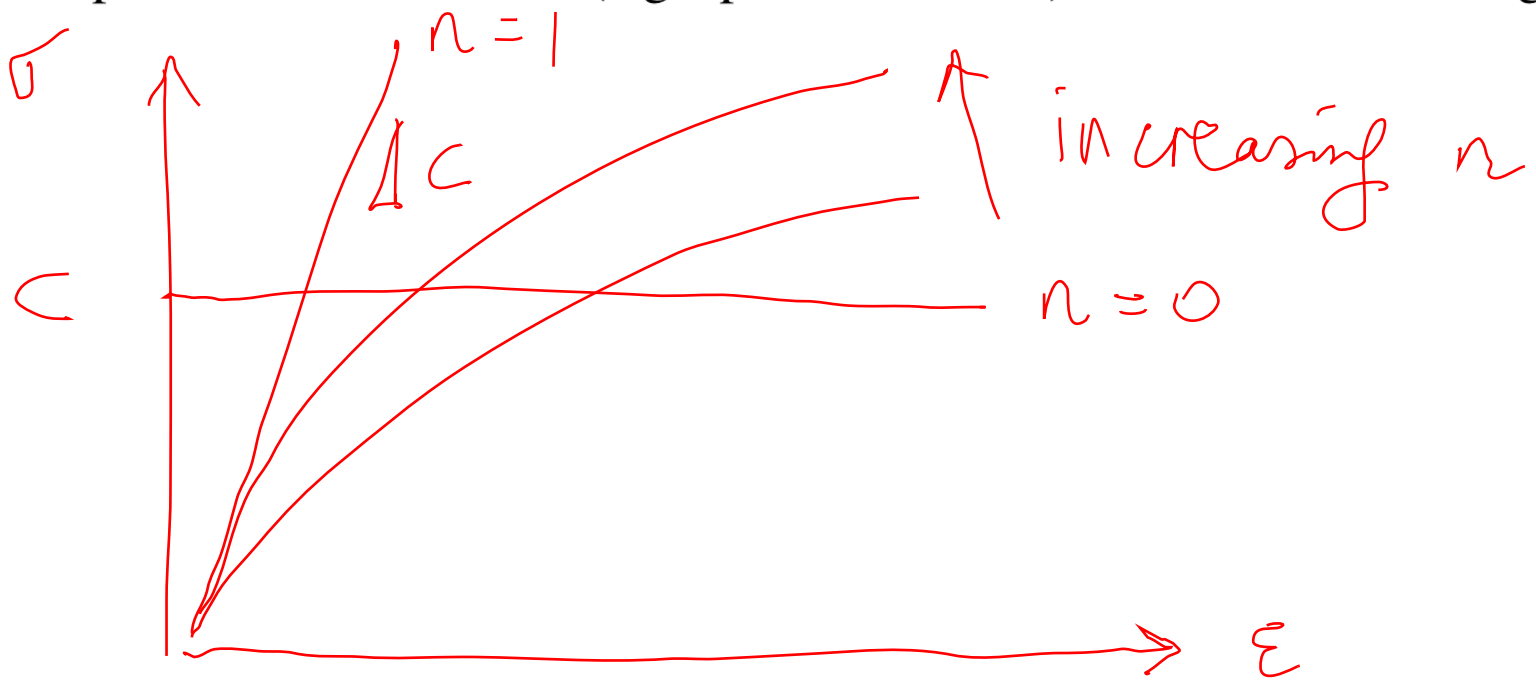

Include a constant term in Ludwik's equation rigid/plastic material.

$$\sigma = Y(1 + m\varepsilon^{n})$$

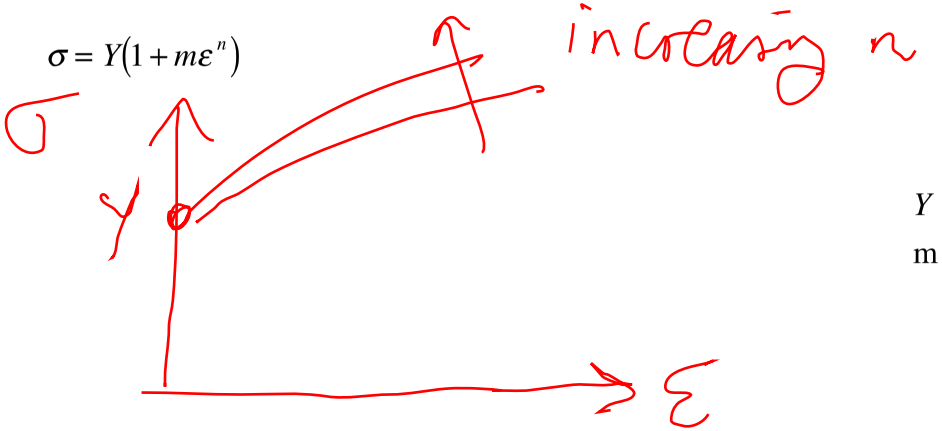

Y = initial yield stress

m and n are constants

n= 1 ; linear hardening.

Generalized power law (Swift). J. Mech. Pys. Solids 1, 1, (1952)

$$\sigma = C(m + \varepsilon)^{n}$$

C, m, n constants.

m = amount of pre-strain for a material whose stress-strain curve corresponds to m = annealed case.

Voce's equation (J. Inst., Metals, 74, 537 (1948) Vocé)

$$\sigma = C\left(1 - me^{-n\varepsilon}\right)$$

e = exponential

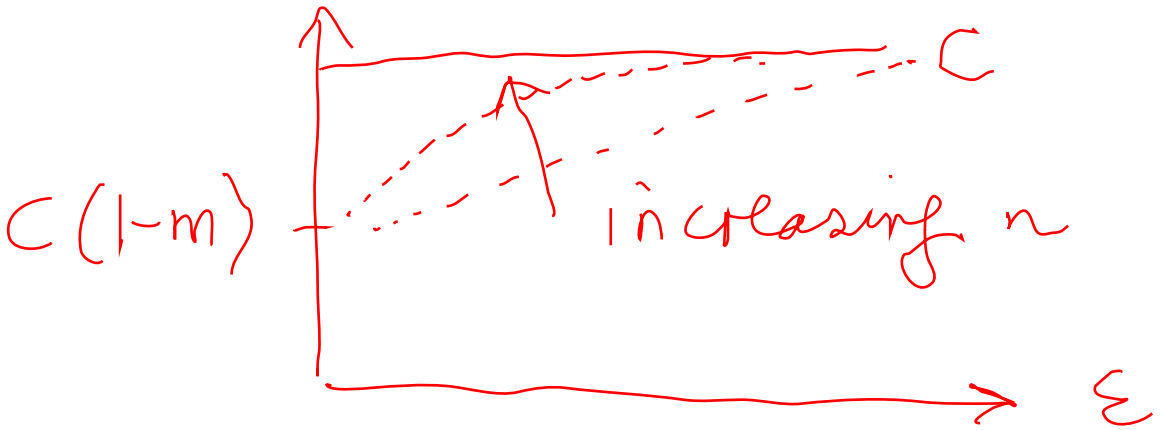

as $\varepsilon \to \infty$ $\sigma = C$.

n = rapidity at which the asymptotic value is reached.

m = state of hardening

= 0 (fully hardened)

Slope of σ vs ε curve $= n(C - \sigma)$ which varies linearly with stress.

At $\varepsilon = 0; \sigma = C(1 - m)$

Tanh $\sigma - \varepsilon$ curve (suggested by Prager)

$$\sigma = \mathrm{Y} \tanh \left[\frac{\mathrm{E}\varepsilon}{\mathrm{Y}} \right].$$

$\sigma - \varepsilon$ curve has an initial slope of E.

As $\varepsilon \to \infty \quad \sigma \to Y$ in an asymptrotic manner

$\varepsilon = 0 \qquad \sigma = 0$

σ is within 1% of Y when $\varepsilon = \frac{4Y}{E} or \frac{E\varepsilon}{Y} = 4.$

$$Tangent \text{ mod } ulus = E\left(1 - \frac{\sigma^2}{Y^2}\right).$$

$$\text{Plastic modulus} = E\left(\frac{Y^2}{\sigma^2} - 1\right).$$

Ramberg - Osgood relationships

Most commonly used $\sigma - \varepsilon$ representation.

$$\varepsilon = \frac{\sigma}{E}\left[1 + \alpha\left(\frac{\sigma}{\sigma_o}\right)^{m-1}\right]$$

σ_o = *yield stress*

$\alpha = cons\tan t$

Advantages of Ramberg - Osgood is that it allows for representation of s - e curve where e and plastic strain are comparable.

Note: $m - 1 = \frac{1}{n} \qquad m = \frac{1}{n} + 1$

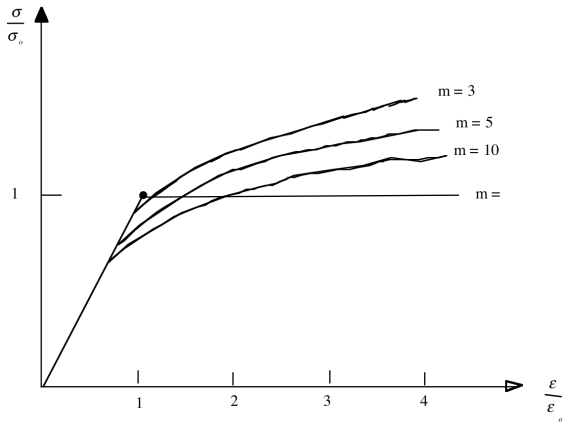

Slope of stress strain curve decreases from E at origin as strain is increased.

At $\sigma = \sigma_o$; plastic strain = α. elastic strain. Secant modulus= dσ/dε = E/(1+α) at σ = e

Tangent Modulus:

$$\frac{1}{T} = \frac{1}{E} + \underbrace{\frac{\alpha m}{E}\left(\frac{\sigma}{\sigma_o}\right)^{m-1}}$$

$1/H$ Plastic modulus

(1970's and beyond) Bodner, et al., J. Appl. Mech., 42, 1975, 385-389

Bodner:

K = measure of strength

$\dot{\varepsilon}_{ij} = \dot{\varepsilon}^{e}_{ij} + \dot{\varepsilon}^{in}_{ij}$ = total strain rate

Definition (Deviatoric Stress: $S_{ij} = \sigma_{ij} - \frac{1}{3}\sigma_{kk}\delta_{ij}$)

$$\dot{\varepsilon}^{in}_{ij} = f\left(\frac{K^2}{J_2}\right) S_{ij}$$

$$f\left(\frac{K^2}{J_2}\right) = \left(\frac{D_o^2}{J_2}\exp\left[-\left(\frac{n+1}{n}\right)\left(\frac{K^2}{3J_2}\right)^n\right]\right)^{0.5}$$

$$\dot{K} = m\left(K_1 - K\right)\dot{W}^{in}$$

Uniaxial Case :

$S_{11} = \frac{2}{3}\sigma\,;\; J_2 = \frac{\sigma^2}{3}$ $\dot{W}^{in} = \sigma.\dot{\varepsilon}^{in}$	$\dot{\varepsilon}^{in} = \frac{2}{3}.\sigma\left(\frac{D_o^{\,2}}{\frac{1}{3}\sigma^2}\exp\left[-\left(\frac{n+1}{n}\right).\left(K^2/\sigma^2\right)^n\right]\right)^{0.5}$ $K = K(W^{in}) = K_1 - (K_1 - K_0).\exp(-mW^{in})$

$D_o, m, A, r, \Delta H, R, n$, K_o are material constants.

S. R. Bodner
Professor.

Y. Partom
Adjunct Associate Professor.

Department of Materials Engineering,
Technion-Israel Institute of Technology,
Haifa, Israel

Constitutive Equations for Elastic-Viscoplastic Strain-Hardening Materials[1]

A set of constitutive equations has been formulated to represent elastic-viscoplastic strain-hardening material behavior for large deformations and arbitrary loading histories. An essential feature of the formulation is that the total deformation rate is considered to be separable into elastic and inelastic components which are functions of state variables at all stages of loading and unloading. The theory, therefore, is independent of a yield criterion or loading and unloading conditions. The deformation rate components are determinable from the current state which permits an incremental formulation of problems. Strain hardening is considered in the equations by introducing plastic work as the representative state variable. The problem of tensile straining has been examined for a number of histories that included straining at various rates, rapid changes of strain rate, unloading and reloading, and stress relaxation. The calculations were based on material constants chosen to represent commercially pure titanium. The results are in good agreement with corresponding experiments on titanium specimens.

Introduction

In an earlier paper [1],[2] the authors proposed an elastic-viscoplastic representation that is suitable for large deformations and general straining histories. The basis of the formulation is the separation of the total deformation rate into elastic (geometrically reversible) and inelastic (geometrically irreversible) components that are functions of state variables and the deformation at all stages of loading and unloading. The theory, therefore, does not require a yield criterion or loading and unloading conditions. The response of the system is calculated on a step-by-step basis and does not depend on reference integration from the "zero" state or the introduction of "memory" functions. Strain hardening was not considered in [1] so the resulting equations are applicable for coupled elastic-perfectly plastic behavior that is strain-rate dependent.

The present paper extends the constitutive equations developed in [1] to include strain hardening by introducing plastic work as the measure of the hardened state. The equation between the inelastic component of the deformation rate and the stress is modified so that the inelastic deformation rate component decreases with increasing plastic work. The assumptions of isotropy and isothermal conditions are maintained in this formulation although strain hardening is known to induce anisotropy.

Problems of variable straining histories of uniaxial tension were analyzed in detail to demonstrate the theory. In general, the constitutive equations are combined with the equilibrium equations (quasi-static and isothermal), and the equations are then solved for the particular boundary conditions. The solution of the relatively simple problem of a cylindrical rod or flat strip subjected to an imposed velocity at one end leads to the force-elongation relation as obtained on a standard testing machine. An essential feature of this formulation is that the uniaxial stress-strain curve at a constant extension rate is obtained as the solution of a boundary-value problem and is not a basic material property.

The basic material properties are the constants appearing in the constitutive equations. These can be chosen for a particular material to best fit test results at two constant rates of extension. It was decided to work with commercially pure titanium because of its relatively high strain-rate sensitivity [2] and its engineering interest, even though it does not experience extensive strain hardening. The strain rate and strain-hardening properties of titanium are fairly well exhibited in the ranges covered by a standard testing machine. Once the material constants are determined, computer calculations can be performed for arbitrary straining histories. In

[1] The research reported in this paper has been sponsored in part by the Air Force Office of Scientific Research (AFSC) through the European Office of Aerospace Research, EOAR, United States Air Force under Grant AFOSR 74-2607.

[2] Numbers in brackets designate References at end of paper.

Contributed by the Applied Mechanics Division for publication in the JOURNAL OF APPLIED MECHANICS.

Discussion on this paper should be addressed to the Editorial Department, ASME, United Engineering Center, 345 East 47th Street, New York, N.Y. 10017, and will be accepted until August 15, 1975. Discussion received after this date will be returned. Manuscript received by ASME Applied Mechanics Division, March, 1974; final revision, June, 1974. Paper No. 75-APM-A.

the present paper, computed results are given for various constant and changing extension rates and for histories that include loading and unloading. The case of stress relaxation is also examined. In all these cases, the computed predictions are compared to results obtained for titanium specimens on an Instron testing machine for the corresponding circumstances.

The calculations and experiments reported in this paper are limited to the case where the stress does not change the sign although the formulation and procedure are generally applicable. Preliminary experiments on cyclic loading in the inelastic range show certain characteristics which are not deducible from the present form of the constitutive equations. Certain modifications of the equations are required to adequately represent cyclic loading behavior.

Analytical Formulation

The general formulation is based upon separation of the total deformation rate d_{ij} into elastic (reversible) and plastic (irreversible) components at all stages of deformation:

$$d_{ij} = d_{ij}^{e} + d_{ij}^{p} \tag{1}$$

where d_{ij} is the symmetric part of the velocity gradient,

$$d_{ij} = (1/2)(v_{i,j} + v_{j,i}) \tag{2}$$

The elastic deformation rate can be related to the stress rate through a strain energy function. In the present formulation, anelastic stresses required to overcome internal viscous mechanisms are not considered and the total stress is taken to be fully elastic.

The plastic deformation rate is assumed to be related to the stress through the flow rule of classical plasticity. This satisfies positive work dissipation requirements and is an assumption within the present framework which is independent of a yield condition. The flow rule can be expressed as

$$d_{ij}^{p} = \underset{\sim}{d}_{ij}^{p} = \lambda \underset{\sim}{\sigma}_{ij} \tag{3}$$

where the bar symbol indicates the deviator. Squaring (3) gives

$$\lambda^2 = D_2^p / J_2 \tag{4}$$

where D_2^p is the second invariant of the plastic deformation rate deviator,

$$D_2^p = (1/2)\underset{\sim}{d}_{ij}^{p}\underset{\sim}{d}_{ji}^{p} \tag{5a}$$

and J_2 is the second invariant of the stress deviator

$$J_2 = (1/2)\underset{\sim}{\sigma}_{ij}\underset{\sim}{\sigma}_{ji} \tag{5b}$$

A principal feature of the present viscoplastic theory is the consideration that D_2^p is a function of J_2. This hypothesis is partially motivated by the extensive work in the field of "dislocation dynamics" which has shown that the dislocation velocity and therefore the uniaxial plastic strain rate is a function of the stress. Since D_2^p is the measure of the "effective" inelastic shear deformation rate and J_2 is the effective shear stress, the statement

$$D_2^p = f(J_2) \tag{6}$$

can be considered to be a multidimensional generalization of the uniaxial result. The particular forms of equation (6) that seem applicable are those used to relate dislocation velocity with stress. In those equations, the dislocation velocity is represented as a power function or as an exponential function of the stress [3]. Similar forms for equation (6) have been proposed and discussed in [1, 4] for the case of no strain hardening. Equation (6) could then be combined with equations (3) and (4) to determine the plastic deformation rate for any given stress.

A form for equation (6) that allows for flexibility in modeling actual material response and has a physical basis is

$$D_2^p = D_0^2 \exp\left[-(A^2/J_2)^n\right] \tag{7}$$

where

$$A^2 = (1/3)Z^2\left(\frac{n+1}{n}\right)^{1/n} \tag{7a}$$

This equation was proposed and discussed in a preliminary report of the present theory [5]. A recent paper [6] suggests the use of a similar expression for the plastic strain rate in a more classical context and discusses some of the metallurgical and mechanical implications.

The material constants for equation (7) are D_0^2, n, and Z. The constant D_0^2 is the bound on D_2^p for large J_2 and influences the rate sensitivity, n is related to the steepness of the curve and therefore to the sharpness of yielding and also to the rate-sensitivity, and Z corresponds in a general way to the yield stress since the maximum slope occurs at $J_2 = Z^2/3$. There is, however, no direct correspondence between Z and the usual definitions of yield stress. The preferred functional form of equation (6) for a particular material would be essentially empirically based and any monotonically increasing function of D_2^p with J_2 is admissible.

Work hardening corresponds to increased resistance to plastic flow which means that D_2^p should vary inversely with the measure of strain hardening. The most significant and simplest state variable to represent this property for straining histories having a constant sign of the stress is the plastic work, W_p, e.g., [7]. An alternate proposal, the integrated plastic strain, is not suitable for viscoplastic materials as it does not reflect the influence of the stress dependence on strain rate.

For D_2^p given by equation (7) to be a decreasing function of W_p, it is possible to set $D_0 = D_0(W_p)$ or $Z = Z(W_p)$. The latter seems to have a sounder physical basis and Z was taken to have the form

$$Z = Z_1 + (Z_0 - Z_1)\exp(-mW_p/Z_0) \tag{8}$$

where Z_0 and Z_1 and m are new material constants. A finite upper limit for Z is required since otherwise D_2^p would approach zero for large W_p. This would correspond to fully elastic behavior and an upward turning stress-strain curve at large strains which is unrealistic. A nonzero value of D_2^p for large W_p leads to the slope of the stress-strain curve approaching zero as the strains become large.

The proposed strain-hardening law corresponds to isotropic hardening and therefore would not characterize the Bauschinger effect. To do this requires that the equation for D_2^p alters upon a change of sign of the characteristic stress. This problem will be treated in detail in subsequent work. Other modifications to the constitutive equations could be made to account for special metallurgical effects such as strain ageing and age hardening. These would involve introducing the time as an explicit parameter in the equation for D_2^p.

Uniaxial Stress Condition

The general procedure for incorporating the proposed constitutive equations into boundary-value problems is given in [1]. The present discussion is limited to the case of uniaxial straining of a simple rod. In order to compare the calculated predictions directly with experimental results, it is necessary to use the same degree of approximation inherent in the experimental measurements. The axial strain in the specimen rod was measured by an Instron extensometer which was limited to 10 percent strain and was calibrated based on a fixed gauge length. For consistency, the simple linear strain measure was used for the present calculations although the method can be based on any nonlinear strain measure. Since the total strains considered are not large, the standard form of Hooke's law is adequate for the elastic stress-strain relation,

$$\underset{\sim}{\sigma}_{ij} = 2G\underset{\sim}{\epsilon}_{ij} \tag{9}$$

$$\sigma_{kk} = 3K\epsilon_{kk} \tag{10}$$

In this example the axial stress $\sigma_x = \sigma$ is the only nonzero component so that equation (7) becomes

$$D_2^p = D_0^2 \exp\left[-(3A^2/\sigma^2)^n\right] \tag{11}$$

and the deviatoric inelastic deformation rates, from equations (4), (5), and (11) are

$$\underline{d}_x^p = \lambda \underline{\sigma}_x = \frac{2D_0}{\sqrt{3}} \circ \frac{\sigma}{|\sigma|} \exp\left[-(1/2)(3A^2/\sigma^2)^n\right] \tag{12}$$

$$\underline{d}_y^p = \underline{d}_z^p = -(1/2)\underline{d}_x^p \tag{13}$$

For an imposed longitudinal velocity $V_c(t)$ on the specimen rod, the axial deformation rate is

$$d_x = \frac{dV_x}{dx} = \frac{V_c}{L} \tag{14}$$

where L is the reference gauge length. The transverse deformation rates, $d_y = d_z$, are determined from the constitutive equations for a given stress level. As shown by equation (1), the deformation rates have both elastic and inelastic components where the elastic components are obtained from the time derivatives of equation (9) and (10) and the inelastic components are given by equations (12) and (13). Although the deformation rate is not, in general, equal to the strain rate, [1], the identity holds for the case of small strains considered for the present examples.

Another simplification due to the limitation to small strains is the direct correspondence of the applied force measured by the load cell and the stress. Since the deformations are fully determined at each stage, the actual force-stress relation could be calculated if necessary.

The rate of plastic work for this case is given by

$$\dot{W}_p = \sigma_x \underline{d}_x^p \tag{15}$$

The preceding equations are adequate to determine the response of the rod to any general imposed velocity $V_c(t)$ such as could be programmed on a testing machine.

Numerical Scheme

A numerical scheme was devised to determine the stress at each stage of the deformation process for given material constants and imposed velocity $V_c(t)$. An incremental procedure was used to determine the changes from the preceding known state over a time interval Δt. This procedure corresponds, in principle, to history and memory effects being essentially incorporated into the state variables and deformation of the current reference state.

The computational method consists of determining at each time increment the stress consistent with the imposed axial deformation rate, equation (14), and the constitutive equations. Starting from a reference state, a value for σ is assumed for the next time increment. The elastic strains and the inelastic strain rates are then calculated from the constitutive equations. The elastic strain rates would be the difference between the new calculated strains and the preceding values divided by the time increment. The elastic and inelastic strain rates are then combined to determine d_x which should agree with equation (14). If not, the value of σ is altered and the calculations repeated in an iterative manner until agreement is established. The procedure is then repeated for the next time increment. The computational method can also be inverted with the transverse deformation rate becoming the iterated quantity. The preferred numerical method would depend on whether the deformation or the stress were prescribed.

The numerical scheme can be readily programmed on a computer and the imposed velocity V_c can be any arbitrary function of time. Changing the strain rate during the course of a test would correspond to changing V_c at a particular time. Unloading would correspond to changing the sign of V_c until the stress reached zero. Stress relaxation results from setting and holding $V_c = 0$, and the creep condition could be realized by varying V_c with time so as to lead to a constant stress. Since the results of the calculations can be programmed for graphical display, there is a direct correspondence of the instructions and results between the computer and the mechanical testing machine. In both cases either the axial velocity or the applied force history is prescribed and the consequent relations of stress-strain, stress-time, or strain-time are obtained.

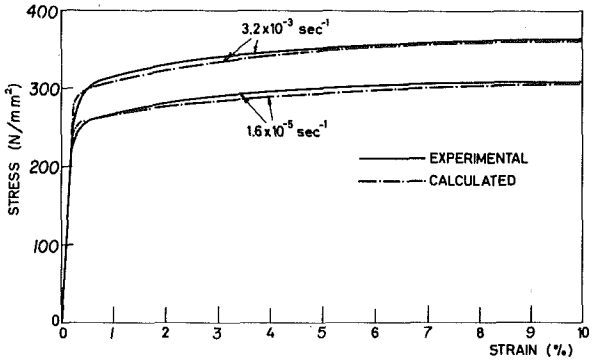

Fig. 1 Experimental and calculated (fitted) stress-strain curves for titanium at constant strain rates

Calculated and Experimental Results

An experimental program was conducted in which specimens of commercially pure titanium were subjected to various straining histories in a 10 ton capacity Instron machine. The machine and measuring system could be considered to be completely rigid for the present experiments. The specimens were all cut from the same 1 mm thick plate in the rolling direction and were 8 mm wide. The plate material was RMI-40 (Reactive Metals Corp.) and was received in the annealed state. No subsequent heat-treatment was performed. The chemical composition as given by the supplier is as follows:

	C	N	H	Fe	O	Mn	Ti
wt percent:	0.1–0.2	0.07	0.015	0.3	0.15	0.2	remainder

The average grain size was relatively large and was about 50 μm. This material is similar to Ti-50A whose properties are listed in handbooks.

An Instron extensometer was used for the strain measurement and the load was recorded as a function of the strain. The basic crosshead velocities employed were 0.005, 0.05, 0.5, and 1.0 cm/min which, for an effective overall gauge length of 5.2 cm, correspond, respectively, to strain rates of 1.6×10^{-5}, 1.6×10^{-4}, 1.6×10^{-3}, and 3.2×10^{-3} sec^{-1}. The material constants for the viscoplastic law were determined by fitting computed stress-strain curves to the experimental ones at the slowest and fastest rates. This led to the following values:

$$\begin{aligned} Z_0 &= 11.5\ K\text{bars}\ (1150\ \text{N/mm}^2) \\ Z_1 &= 14.0\ K\text{bars}\ (1400\ \text{N/mm}^2) \\ D_0^2 &= 10^8\ \text{sec}^{-2} \\ n &= 1 \\ m &= 100 \end{aligned}$$

The elastic constants for titanium are

$$\begin{aligned} K &= 1.23 \times 10^3\ K\text{bars}\ (1.23 \times 10^5\ \text{N/mm}^2) \\ G &= 0.44 \times 10^3\ K\text{bars}\ (0.44 \times 10^5\ \text{N/mm}^2) \end{aligned}$$

The resulting fits for the computed and experimental stress-strain curves at the slowest and fastest rates are shown in Fig. 1. It is noted that the inclusion of strain hardening in the analysis is important even for this material since otherwise the calculated curves would be flat after the initial yield region, i.e., after about 1 percent strain.

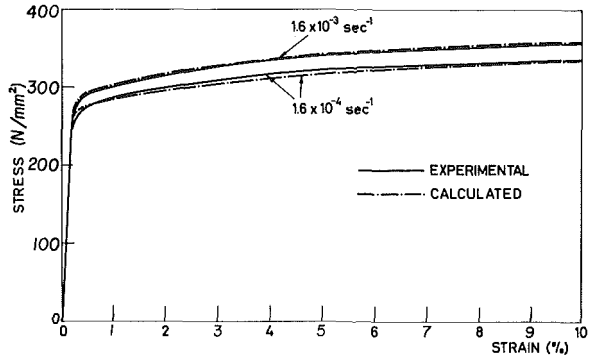

Fig. 2 Experimental and calculated (derived) stress-strain curves for titanium at constant strain rates

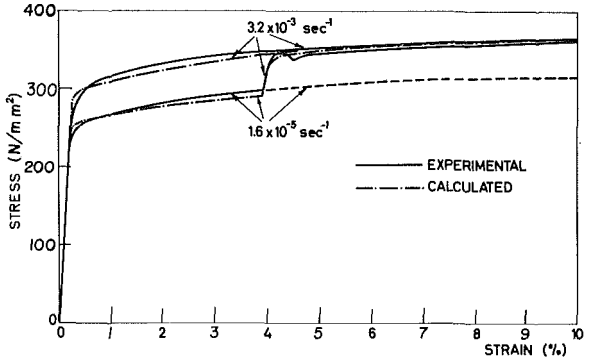

Fig. 3 Experimental and calculated stress-strain curves for titanium subjected to a rapid change (increase) in strain rate

The importance and value of the constitutive equations are, of course, the extent to which they can predict the consequences of complex straining histories that are different from the ones used to obtain the material constants. A series of experiments and corresponding calculations were performed to examine the overall validity of the representation. The experiments were based on the capabilities of the Instron machine and were quasi static uniaxial tension tests of titanium sheet specimens. A series of cyclic tension-compression tests were also conducted but will be reported separately.

Test and Calculation Program

1 Constant rate tests were conducted to strains of 10 percent at the intermediate strain rates of 1.6×10^{-4} and 1.6×10^{-3} sec^{-1}.

2 Loading, unloading, and reloading tests were performed at various constant strain rates.

3 Specimens were subjected to rapid changes of strain rate without unloading. One test was to pull the specimen at the fastest rate to 4 percent strain and then to rapidly change to the slowest rate. Alternatively, specimens were pulled at the slowest rate to 4 percent strain and then the rate was changed to the fastest value. The relatively sudden change of strain rate was accomplished by simply pressing the crosshead velocity control button on the Instron which activates a magnetic clutch on the speed regulator. The response times and actions of the clutch and recorder and sufficiently fast and smooth to obtain accurate results without extraneous dynamic effects.

4 Tests with changes of strain rate were also conducted after first unloading the specimens at the 4 percent strain level. These were similar to the previous tests but the specimens were first completely unloaded before the strain rate was changed.

5 Stress relaxation tests were performed in which the specimens were pulled at a constant rate to 10 percent strain after which the crosshead was stopped. The subsequent decrease of load was then observed.

A basic problem in testing commercially pure titanium is the inherent scatter of results even with specimens prepared from the same plate. This is due to the strong influence of small differences in impurities and heat treatment on the initial yield region. Generally, the same kind of test was repeated 4 or 5 times and the average used as the experimental result.

To provide a more complete basis for evaluating the general applicability of the proposed equations, it would be desirable to perform multiaxial stress state experiments on the same material since the material constants should apply for all conditions. Such experiments have not yet been performed and are a necessary extension of this work.

Discussion

The calculated and experimental stress-strain curves for the intermediate rates are shown in Fig. 2. Since the experimental curves of Fig. 1 are in good agreement with the calculated fitted curves, the correspondence indicated in Fig. 2 could be expected.

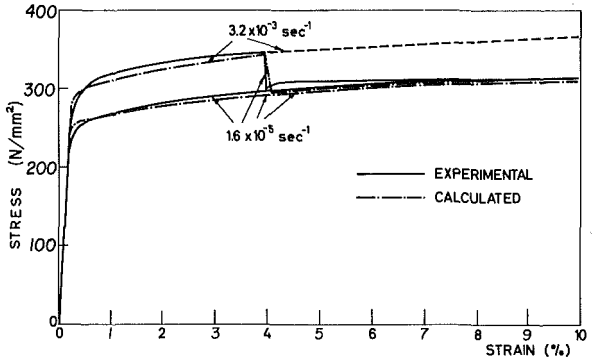

Fig. 4 Experimental and calculated stress-strain curves for titanium subjected to a rapid change (decrease) in strain rate

The cases of rapid changes of strain rate at 4 percent strain are shown in Figs. 3 and 4. For increasing strain rate, Fig. 3, the immediate response of both the experimental and calculated curves is close to elastic after which the curves approach from the low side the value they would have had for a constant strain rate. Similar results for more extreme changes of strain rate have been obtained in shear for titanium [2] and aluminum [8]. The experimental curve shows an upper yield point while the calculated curve is smooth. The upper yield point effect is probably due to detailed material effects, e.g., changes in mobile dislocation density, that are not represented by the constitutive equations. These effects are discussed in the metallurgical literature, e.g., [9, 10]. The subsequent lower stress level at large strains for the calculated curve with the rate change compared to the constant rate case is due to W_p being less prior to the change. This effect would not have resulted had the integrated plastic strain been used as the strain-hardening parameter.

The initial close to elastic response upon change of strain rate is due to the large increase in the elastic deformation rate component. Since the stress level remains the same at the instant of change, the plastic deformation rate remains constant and the overall increased rate is supplied by the elastic component. Prior to the rate change, the plastic deformation rate at 4 percent strain is 99.7 percent of the total while the ratio drops to 56.6 percent immediately upon the change. If the change had been sufficiently rapid for inertia effects to occur, the elastic component would result in an elastic wave being generated while the effect of the inelastic component would rapidly attenuate. This corresponds to the well-known result that a small amplitude pulse applied to a plastically strained medium travels at the elastic wave velocity.

The inverse procedure of rapidly reducing the imposed strain rate leads for both the experimental and calculated curves to unloading that is almost completely elastic and then to a transition to the uniform rate case, Fig. 4. The curves remain above the corresponding uniform rate curves which for the calculated case is due

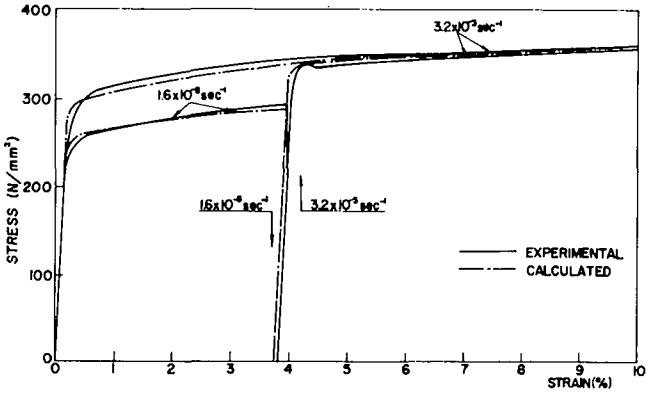

Fig. 5 Experimental and calculated stress-strain curves for titanium subjected to unloading, and subsequent reloading at a faster rate

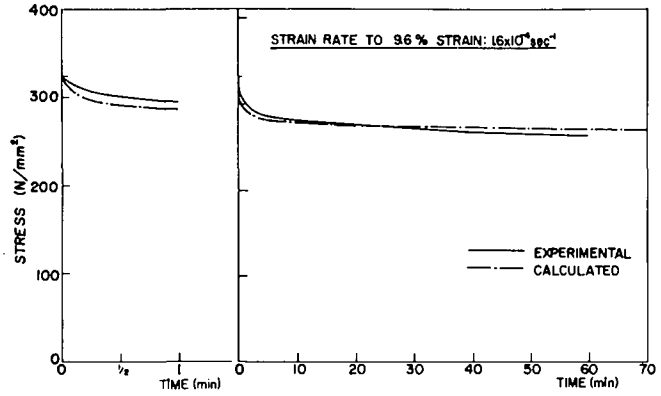

Fig. 6 Experimental and calculated stress relaxation curves for titanium

to the larger initial value of W_p. The experimental curves show a dip and rise analogous to an inverse yield point effect.

Various unloading and reloading tests were performed at both constant and changing strain rates. The case of changing to a higher strain rate upon reloading is shown in Fig. 5. The inelastic contribution to the unloading and most of the reloading sections is small (but nonzero) and therefore those portions of the curves are essentially elastic. The experimental curve shows an upper yield point effect that is less pronounced than in Fig. 3. The calculated curve again follows the experimental one closely but without the upper yield point effect. Similar experimental results, but without the yield point effect, have been obtained for aluminum in shear [11].

An experimental procedure that is basically different from the preceding ones is stress relaxation after extension to 9.6 percent strain. The experimental and calculated results for an initial straining rate of 1.6×10^{-4} sec^{-1} are shown in Fig. 6. The overall correspondence of the results appears to be good although there is some discrepancy in the early time region. An interesting aspect of uniaxial stress relaxation is the relative importance of the multidimensional strain state in the calculations. Imposing the condition that the overall axial strain rate is zero means that the axial elastic strain rate is equal to and opposite the axial plastic strain rate. The elastic strain rate is therefore a negative function of stress through the flow law in the form of equation (12). According to the present formulation, the stress would approach zero asymptotically with time, i.e., the stress would fully relax, although the relaxation rate becomes very small after a short time.

To complete the uniaxial stress cases, it would have been desirable to include some creep experiments. The Instron machine, however, can only approximate constant load by stepwise adjustment of the crosshead, but this is not suitable for accurate results in the viscoplastic range. Since a proper creep machine for the required loads was not available, such tests were not conducted. Using the analytical formulation to compute the time-dependent strain for constant stress would be straightforward.

Uniaxial tension-compression cyclic loading tests were conducted with results similar to those appearing in the literature. The present theoretical formulation could not adequately represent these results as it does not account for the softening observed upon change of the sign of the applied stress. This requires further development of the analysis.

Conclusions

The proposed elastic-viscoplastic theory can adequately represent the actual behavior of a typical rate-sensitive metal for a variety of tensile straining histories. The case of cyclic loading which is important for fatigue studies requires further development of the analysis. The applicability of the theory for multidimensional stress states also requires further investigation.

References

1 Bodner, S. R., and Partom, Y., "A Large Deformation Elastic-Viscoplastic Analysis of a Thick-Walled Spherical Shell," JOURNAL OF APPLIED MECHANICS, Vol. 39, TRANS. ASME, Vol. 94, Series E, 1972, pp. 751–757.

2 Nicholas, T., "Strain Rate and Strain-Rate-History Effects in Several Metals in Torsion," *Experimental Mechanics*, Vol. 11, 1971, pp. 370–374.

3 Gilman, J. J., *Micromechanics of Flow in Solids*, McGraw-Hill, New York, 1969.

4 Bodner, S. R., "Constitutive Equations for Dynamic Material Behavior," *Mechanical Behavior of Materials Under Dynamic Loads*, ed., Lindholm, U. S., Springer-Verlag, New York, 1968, pp. 176–190.

5 Bodner, S. R., and Partom, Y., "Dynamic Inelastic Properties of Materials, Part II—Representation of Time-Dependent Characteristics of Metals," *Proceedings, Eighth Congress of the International Council of the Aeronautical Sciences*, Amsterdam, 1972, ICAS Paper 72-28.

6 Kelly, J. M., and Gillis, P. P., "The Influence of a Limiting Dislocation Flux on the Mechanical Response of Polycrystalline Metals," *International Journal of Solids and Structures*, Vol. 10, 1974, pp. 45–59.

7 Hill, R., *The Mathematical Theory of Plasticity*, Clarendon Press, Oxford, 1950.

8 Frantz, R. A., and Duffy, J., "The Dynamic Stress-Strain Behavior in Torsion of 1100-0 Aluminum Subjected to a Sharp Increase in Strain Rate," JOURNAL OF APPLIED MECHANICS, Vol. 39, TRANS. ASME, Vol. 94, Series E, 1972, pp. 939–945.

9 Orava, R. N., Stone, G., and Conrad, H., "The Effects of Temperature and Strain Rate on the Yield and Flow Stresses of α-Titanium," *Transactions of the American Society of Metals*, Vol. 59, 1966, pp. 171–184.

10 Santhanam, A. T., Ramachandran, V., and Reed-Hill, R. E., "An Investigation of the Shape of the Titanium Stress Strain Curves After a Strain Rate Change," *Metallurgical Transactions*, Vol. 1, 1970, pp. 2593–2598.

11 Klepaczko, J., "Strain Rate History Effects for Polycrystalline Aluminum and Theory of Intersections," *Journal of the Mechanics and Physics of Solids*, Vol. 16, 1968, pp. 255–266.

Mechanical Threshold Stress (MTS) Model

$$\frac{\sigma}{\mu} = \frac{\sigma_a}{\mu} + s_i\left(\dot{\varepsilon},T\right)\frac{\hat{\sigma}_i}{\mu_o} + s_\varepsilon\left(\dot{\varepsilon},T\right)\frac{\hat{\sigma}_\varepsilon}{\mu_o}$$

$$s_i = \left\{1 - \left[\frac{kT}{g_{oi}\mu b^3}\ln\left(\frac{\dot{\varepsilon}_{oi}}{\dot{\varepsilon}}\right)\right]^{1/q_i}\right\}^{1/p_i}$$

$$s_\varepsilon = \left\{1 - \left[\frac{kT}{g_{o\varepsilon}\mu b^3}\ln\left(\frac{\dot{\varepsilon}_{o\varepsilon}}{\dot{\varepsilon}}\right)\right]^{1/q_\varepsilon}\right\}^{1/p_\varepsilon}$$

Essentially the stress is decomposed into multiple parts.

The first term is the athermal component of stress

The next two terms represent the initial hardening (yielding)

$$\frac{\sigma_a}{\mu} + s_i\left(\dot{\varepsilon}, T\right)\frac{\hat{\sigma}_i}{\mu_o}$$

The third term represents the hardening behavior (dislocation Interactions) and saturation stress.

$$s_\varepsilon\left(\dot{\varepsilon}, T\right)\frac{\hat{\sigma}_\varepsilon}{\mu_o}$$

Shear Modulus Variation

$$\mu(T) = \mu_o - \frac{D_o}{\exp\left(\frac{T}{T_o}\right) - 1}$$

When only characterizing the yield behavior of the material, the third term in equation B.1 can be ignored. Substituting in for S_i results in the form

$$\frac{\sigma_y - \sigma_a}{\mu} = S_i\left(\dot{\epsilon}, T\right)\frac{\hat{\sigma}_i}{\mu_0} = \left[1 - \left(\frac{kT}{g_{0i}\mu b^3}\ ln\frac{\dot{\epsilon}_0}{\dot{\epsilon}}\right)^{1/q_i}\right]^{1/p_i}\frac{\hat{\sigma}_i}{\mu_0} \tag{B.3}$$

The equation which is the basis for the Fisher plot is given below

$$\left(\frac{\sigma_y - \sigma_a}{\mu}\right)^{p_i} = \left[1 - \left(\frac{kT}{g_{0i}\mu b^3}\ ln\frac{\dot{\epsilon}_0}{\dot{\epsilon}}\right)^{1/q_i}\right]\left(\frac{\hat{\sigma}_i}{\mu_0}\right)^{p_i} \tag{B.4}$$

rearranging

$$\left(\frac{\sigma_y - \sigma_a}{\mu}\right)^{p_i} = \left(\frac{\hat{\sigma}_i}{\mu_0}\right)^{p_i} - \left[\frac{kT}{g_{0i}\mu b^3}\ ln\frac{\dot{\epsilon}_0}{\dot{\epsilon}}\right]^{1/q_i}\left(\frac{\hat{\sigma}_i}{\mu_0}\right)^{p_i} \tag{B.5}$$

Writing in slope intercept form,

$$\left(\frac{\sigma_y - \sigma_a}{\mu}\right)^{p_i} = -\left(\frac{1}{g_{0i}}\right)^{1/q_i}\left(\frac{\hat{\sigma}_i}{\mu_0}\right)^{p_i} \cdot \left[\left(\frac{kT}{\mu b^3}\ ln\frac{\dot{\epsilon}_0}{\dot{\epsilon}}\right)^{1/q_i}\right] + \left(\frac{\hat{\sigma}_i}{\mu_0}\right)^{p_i} \tag{B.6}$$

The relation to slope intercept form is given below and plotted in Figure 2.5.

$$y = m \cdot [x] + b \tag{B.7}$$

Analyzing Data (first we ignore the last term)

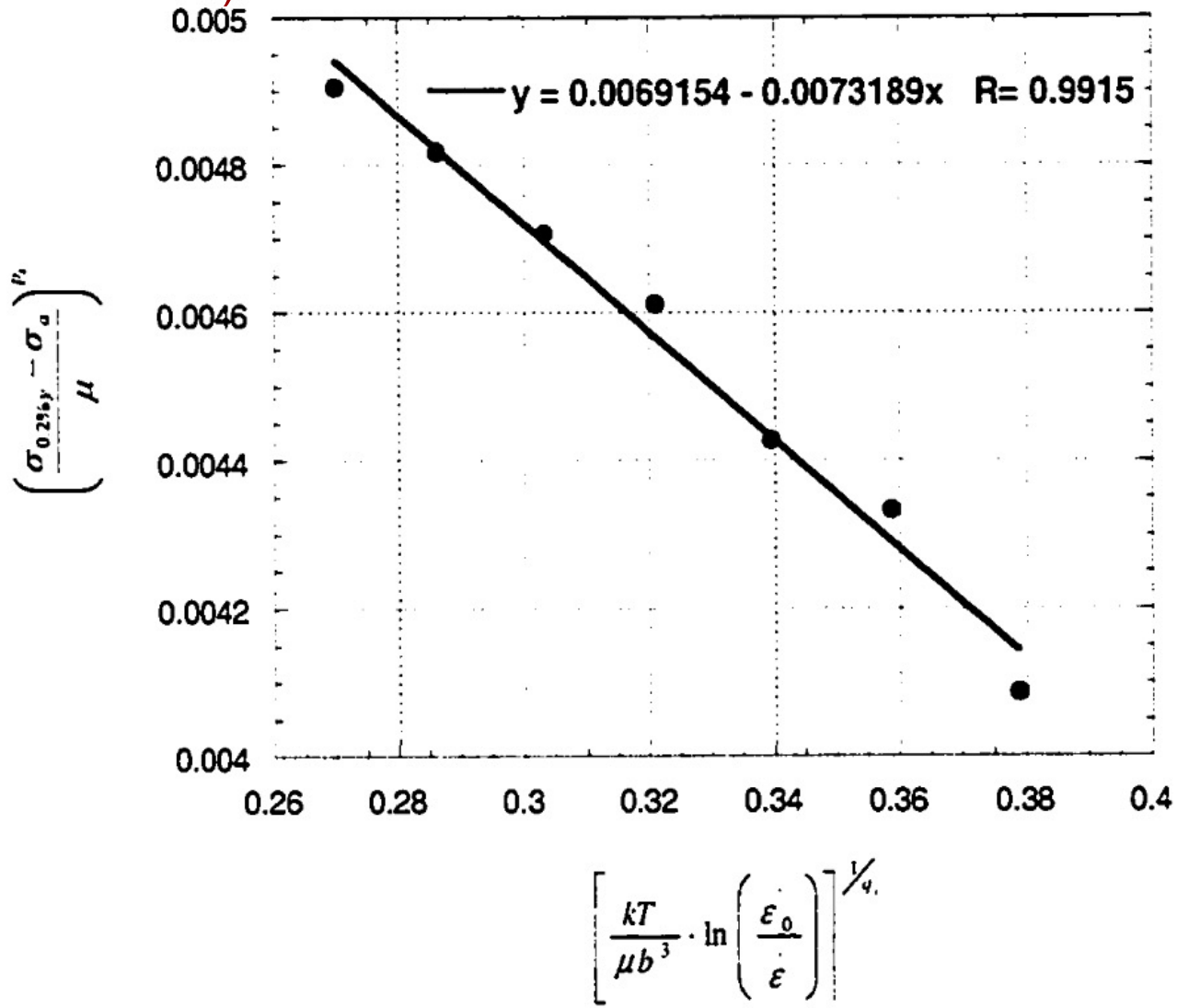

Figure 2.5 Fisher plot for AA 5182 used to determine the values for $\hat{\sigma}_i$ and g_{0i}. These values were determined to be 199 MPa and 0.945, respectively. For this plot, the best correlation coefficient resulted when the values of p_i and q_i were equal to 1. The yield stress was defined using a 0.2 percent offset method.

Analyzing Data (first we ignore the last term)

The kinetic equation becomes:

$$\left(\frac{\sigma-\sigma_a}{\mu}\right)^p = \left\{1-\left[\frac{kT}{g_o\mu b^3}\ln\left(\frac{\dot{\varepsilon}_o}{\dot{\varepsilon}}\right)\right]^{1/q}\right\}\left(\frac{\hat{\sigma}}{\mu_o}\right)^p$$

suggests that yield stress data should be plotted as

$$\left(\frac{\sigma-\sigma_a}{\mu}\right)^p \quad \text{versus} \quad \left[\frac{kT}{\mu b^3}\ln\left(\frac{\dot{\varepsilon}_o}{\dot{\varepsilon}}\right)\right]^{1/q}$$

The slope in this plot can be easily related to g_o.

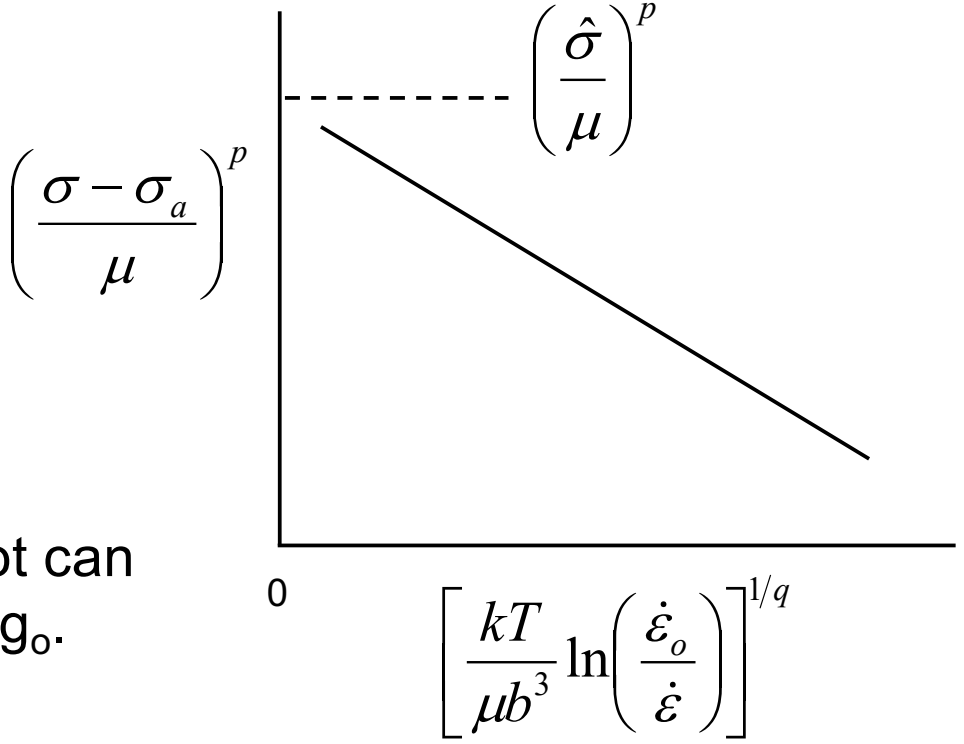

Analyzing Data - Niobium

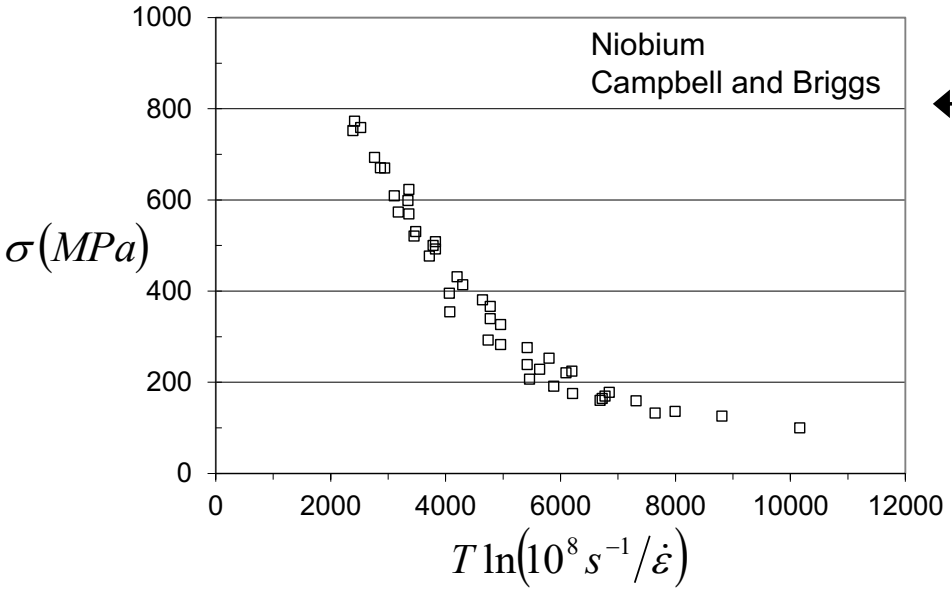

$$\sigma = \left\{1 - \left[\frac{kT}{G}\ln\left(\frac{\dot{\varepsilon}_o}{\dot{\varepsilon}}\right)\right]\right\}\hat{\sigma}$$

$$\left(\frac{\sigma - \sigma_a}{\mu}\right)^p = \left\{1 - \left[\frac{kT}{g_o \mu b^3}\ln\left(\frac{\dot{\varepsilon}_o}{\dot{\varepsilon}}\right)\right]^{1/q}\right\}\left(\frac{\hat{\sigma}}{\mu_o}\right)^p$$

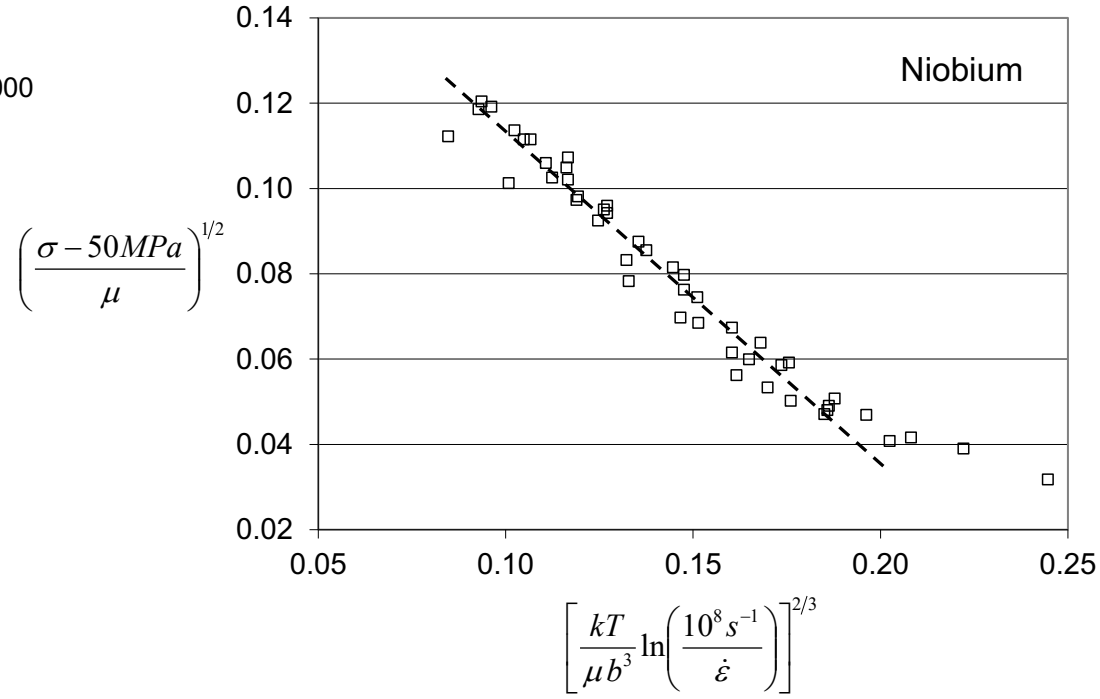

Incorporating the temperature dependent shear modulus and the more descriptive obstacle profile has enabled a more linear correlation.

Next we consider the last term

$$\sigma - \sigma_a - S_i(\dot{\epsilon}, T)\frac{\mu \cdot \hat{\sigma}_i}{\mu_0} = S_\epsilon(\dot{\epsilon}, T)\frac{\mu \cdot \hat{\sigma}_\epsilon}{\mu_0}$$

$$\frac{d\hat{\sigma}_\epsilon/d\epsilon}{\mu} = \frac{\hat{\theta}}{\mu} = \frac{\hat{\theta}_0}{\mu_0}\left(1 - \frac{\hat{\sigma}_\epsilon}{\hat{\sigma}_{\epsilon s}}\right)^\kappa$$

$$\sigma - \sigma_a - \sigma_{yield} = \left[1 - \left(\frac{kT}{g_{0\epsilon}\mu b^3}\ ln\frac{\dot{\epsilon}_0}{\dot{\epsilon}}\right)^{1/q_\epsilon}\right]^{1/p_\epsilon}\frac{\mu \cdot \hat{\sigma}_\epsilon}{\mu_0}$$

$$\left[\frac{\sigma}{\mu} - \frac{\sigma_{yield}}{\mu}\right]^{p_\epsilon} = -\left(\frac{1}{g_{0\epsilon}}\right)^{1/q_\epsilon}\left(\frac{\hat{\sigma}_{\epsilon s}}{\mu_0}\right)^{p_\epsilon} \cdot \left[\frac{kT}{\mu b^3}\ ln\frac{\dot{\epsilon}_{0\epsilon}}{\dot{\epsilon}}\right]^{1/q_\epsilon} + \left(\frac{\hat{\sigma}_{\epsilon s}}{\mu_0}\right)^{p_\epsilon}$$

Choosing a form of the saturation, $\hat{\sigma}_{\epsilon s}$, involving the Fisher parameter

$$\left(\frac{\hat{\sigma}_{\epsilon s}}{\mu}\right)^{p_\epsilon} = -\left(\frac{1}{g_{0\epsilon s}}\right)^{\frac{1}{q_\epsilon}}\left(\frac{\hat{\sigma}_{\epsilon s0}}{\mu_0}\right)^{p_\epsilon}\left[\left(\frac{kT}{\mu b^3}\ ln\frac{\dot{\epsilon}_{0\epsilon s}}{\dot{\epsilon}}\right)^{\frac{1}{q_\epsilon}}\right] + \left(\frac{\hat{\sigma}_{\epsilon s0}}{\mu_0}\right)^{p_\epsilon}$$

Table 2.1 Fitting parameters for the general form of the MTS model optimized for a strain rate of 3.0 s^{-1} and temperatures between 350°C and 500°C. A power-law form of the saturation stress (equation 2.7) was taken from the literature [9].

Parameter	Value	Unit	Parameter	Value	Unit
σ_a	0.0	MPa	θ_0	12500	MPa
$\frac{\sigma_i}{\mu_0}$	0.0069145	–	κ	2	–
g_{oi}	0.945	–	$g_{0\epsilon s}$	0.184	–
$\dot{\epsilon}_{0i}$	10^7	s^{-1}	$\hat{\sigma}_{\epsilon s0}$	1075	MPa
q_i	1.0	–	$\dot{\epsilon}_{0\epsilon s}$	10^7	s^{-1}
p_i	1.0	–	k/b^3	0.5899	MPa/°K
$g_{o\epsilon}$	0.446	–	b	2.86×10^{-10}	m
$\dot{\epsilon}_{0\epsilon}$	10^7	s^{-1}	μ_0	28815	MPa
q_ϵ	1.0	–	D	3440	MPa
p_ϵ	1.0	–	T_0	215	°K

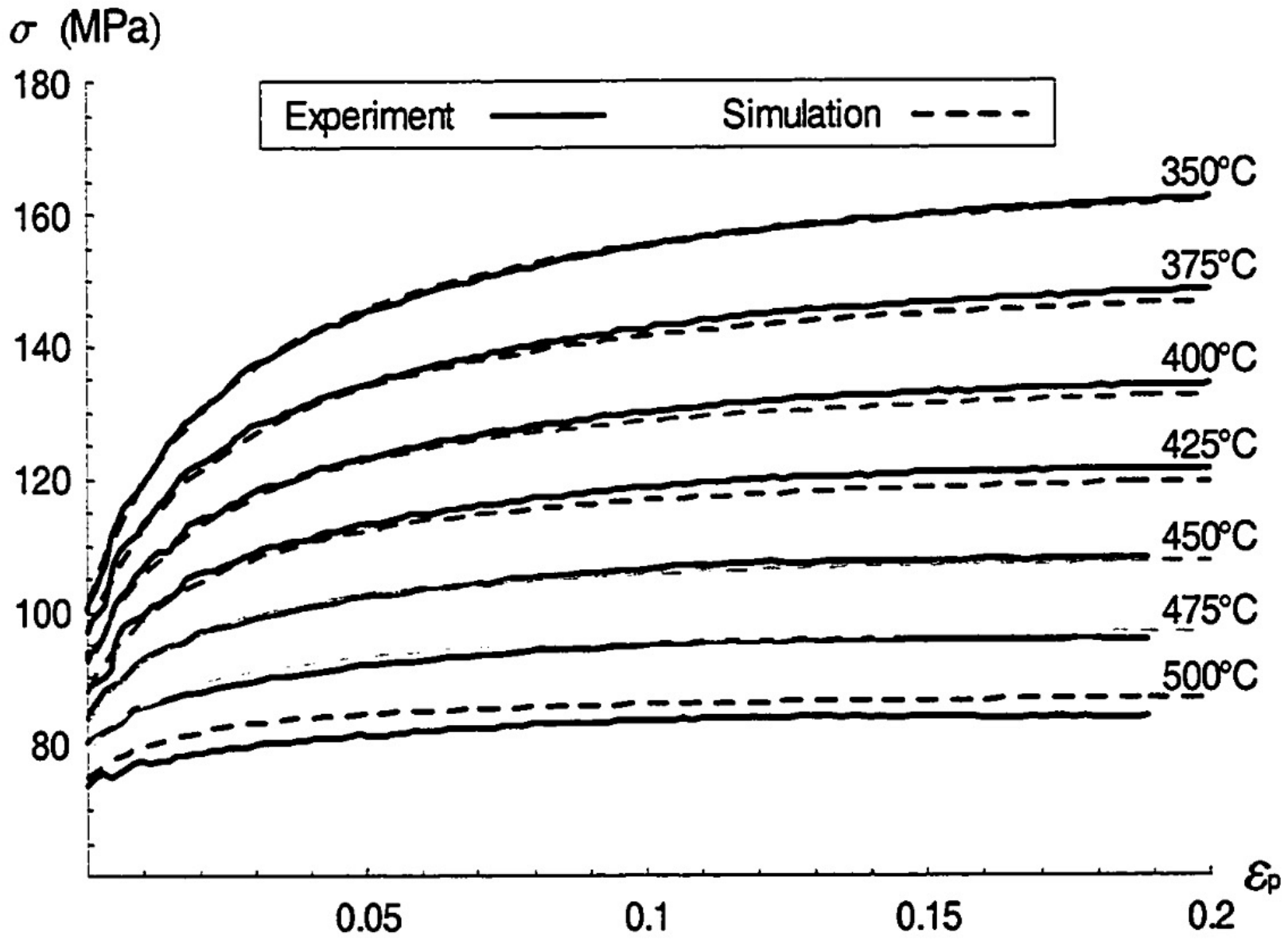
σ (MPa)
180
160
140
120
100
80
Experiment
Simulation
350°C
375°C
400°C
425°C
450°C
475°C
500°C
0.05
0.1
0.15
0.2
εp